Review

Post-graphene 2D materials-based antimicrobial agents: focus on fabrication strategies and biosafety assessments

Jie Zheng[1], Jingchen Li[1], Lihui Zhang[2], Xiaojun Chen[3], Yadong Yu[1,2,*] (iD), and He Huang[1,2]

[1] College of Biotechnology and Pharmaceutical Engineering, Nanjing Tech University, Nanjing 211800, People's Republic of China
[2] School of Food Science and Pharmaceutical Engineering, Nanjing Normal University, Nanjing 210023, People's Republic of China
[3] School of Chemistry and Molecular Engineering, Nanjing Tech University, Nanjing 211816, People's Republic of China

ABSTRACT

Bacterial infections have caused serious threats to public health nowadays because of the generation of antibiotics-resistant bacteria. Recently, new 2D materials beyond graphene (post-graphene 2D materials, pg-2DMs), such as transition metal dichalcogenides, black phosphorus, layered double hydroxides and MXenes, have been intensively explored for antimicrobial applications on account of their superior physiochemical properties. Here, we provide an up-to-date overview of the post-graphene 2D materials-based antimicrobial agents (pg-2DMs-AA), focusing on (1) the strategies to improve the antimicrobial activities of pg-2DMs-AA and (2) the biosafety assessments of pg-2DMs-AA. Finally, insights regarding the current gaps and outlooks for future opportunities in this field are given as well.

Introduction

Bacteria-caused diseases threaten the human health seriously and have turned to be the leading causes of death worldwide [1, 2]. The abuse of antibiotics has led to the increase in drug-resistant bacteria, which makes the battle against bacterial infections even worse [3]. In this context, developing new and effective antibacterial agents is imminent.

Nanomaterials with antimicrobial activities have garnered many attentions both in scientific researches and in industrial applications during the past decades. Comparing with the small molecular antibiotics, antimicrobial nanomaterials generally display better performances in terms of long-lasting antibacterial activities and environmental toxicities. Besides, antimicrobial nanomaterials circumvent the emergences of drug-resistant bacteria, which is a serious problem for the small molecular antibiotics because of their specific targets of action [4]. Recently, post-graphene 2D materials (pg-2DMs), like transition metal dichalcogenides (TMDs), black phosphorus (BP) and layered double hydroxides (LDHs), have been presented as promising candidates to

Address correspondence to E-mail: yadongyu@njtech.edu.cn

combat pathogens [5, 6]. The antibacterial mechanisms of pg-2DMs have been proposed as well, including (1) physical interactions (lipid extraction, "nano-knife" effect, etc.) that will damage cell membrane and block the cell material exchange, (2) photothermal effects and (3) photocatalytic generation of reactive oxygen species (ROS) [5].

The promising potentials of graphene in antimicrobial applications have greatly stimulated the interest of researchers in fabricating various post-graphene 2D materials-based antimicrobial agents (pg-2DMs-AA) (Fig. 1a). Thus far, many pg-2DMs, such as transition metal dichalcogenides (TMDs) [7, 8], black phosphorus (BP) [9, 10] and layered double hydroxides (LDHs) [11], MXenes [12, 13], g-C_3N_4 [14, 15] and In_2Se_3 [16], have been utilized to prepare antimicrobial agents (Fig. 1b). In this review, we overview the methods for enhancing the antimicrobial activities of pg-2DMs-AA and the biosafety assessment of the pg-2DMs-AA.

Strategies to improve the antimicrobial activities of post-graphene 2D materials-based antimicrobial agents

Synthesizing new-generation antibacterial agents based on pg-2DMs is of great interest to scientists and engineers in many fields such as biomedicine and food packing. Due to their natures, pristine pg-2DMs generally display limited antimicrobial activities. Thus, to fabricate efficient antibacterial agents, the first and crucial step is to choose rational strategies to boost the antimicrobial capacities of pg-2DMs-AA. To summarize these strategies, herein we conduct a comprehensive literature survey by inputting keywords (i.e., 2D materials, two-dimensional materials, MoS_2, black phosphorus, g-C_3N_4, antibacterial, antimicrobial, disinfection, sterilization) into the widely used databases (e.g., Web of Science, Scopus, Google Scholar). Notably, we do not intend to summarize all the methods employed in preparing pg-2DMs-AA, but only to introduce the frequently utilized and applicable approaches (Fig. 2).

Fabricating single- or few-layer pg-2DMs

The researches about graphene-like 2D materials are greatly motivated by the unique physicochemical properties of these materials with the reduction in the thickness to single or few layers. In the antimicrobial field, reducing the layers of graphene significantly enhances its antimicrobial activities [17, 18]. In addition to graphene, other 2D materials also show the similar phenomenon [13, 19]. For instance, Yang et al. utilized the Li intercalation approach to prepare the chemically exfoliated few-layer MoS_2 (ce-MoS_2). Compared with the raw MoS_2 powder, ce-MoS_2 demonstrated a much stronger inactivation ability on *Escherichia coli* DH5α (Fig. 3a) [19]. The possible underlying mechanism is the decrease in the 2D materials' layer will generate more atomically sharp edges, more active sites, larger surface to volume ratio and higher photothermal conversion efficiency
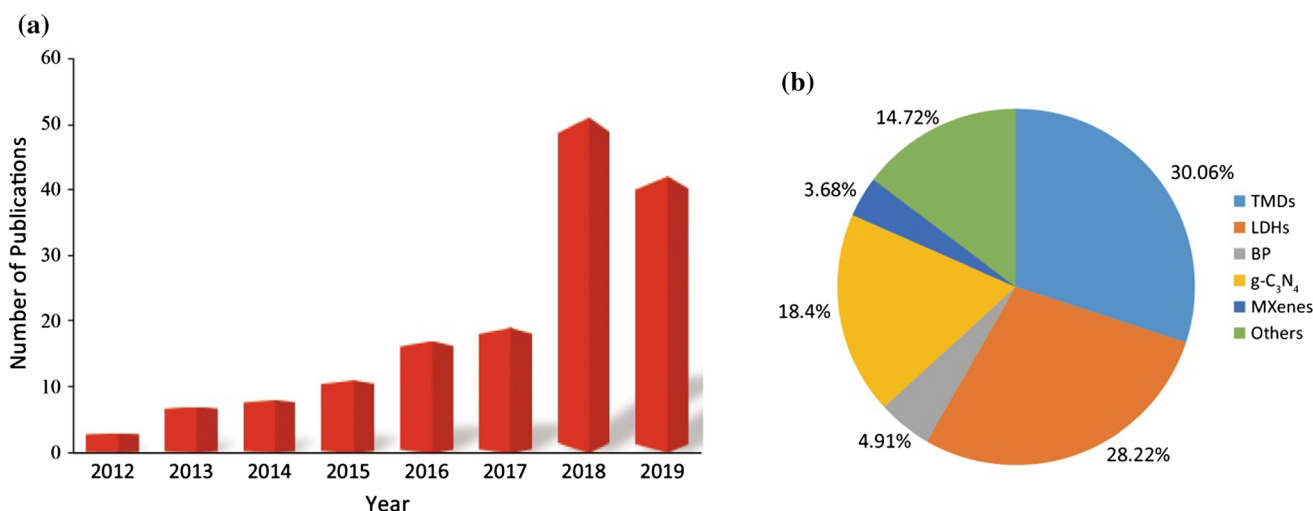

Figure 1 **a** Numbers of pg-2DMs-AA-associated publications; **b** percentages of the pg-2DMs that have been used to prepare antimicrobial agents.
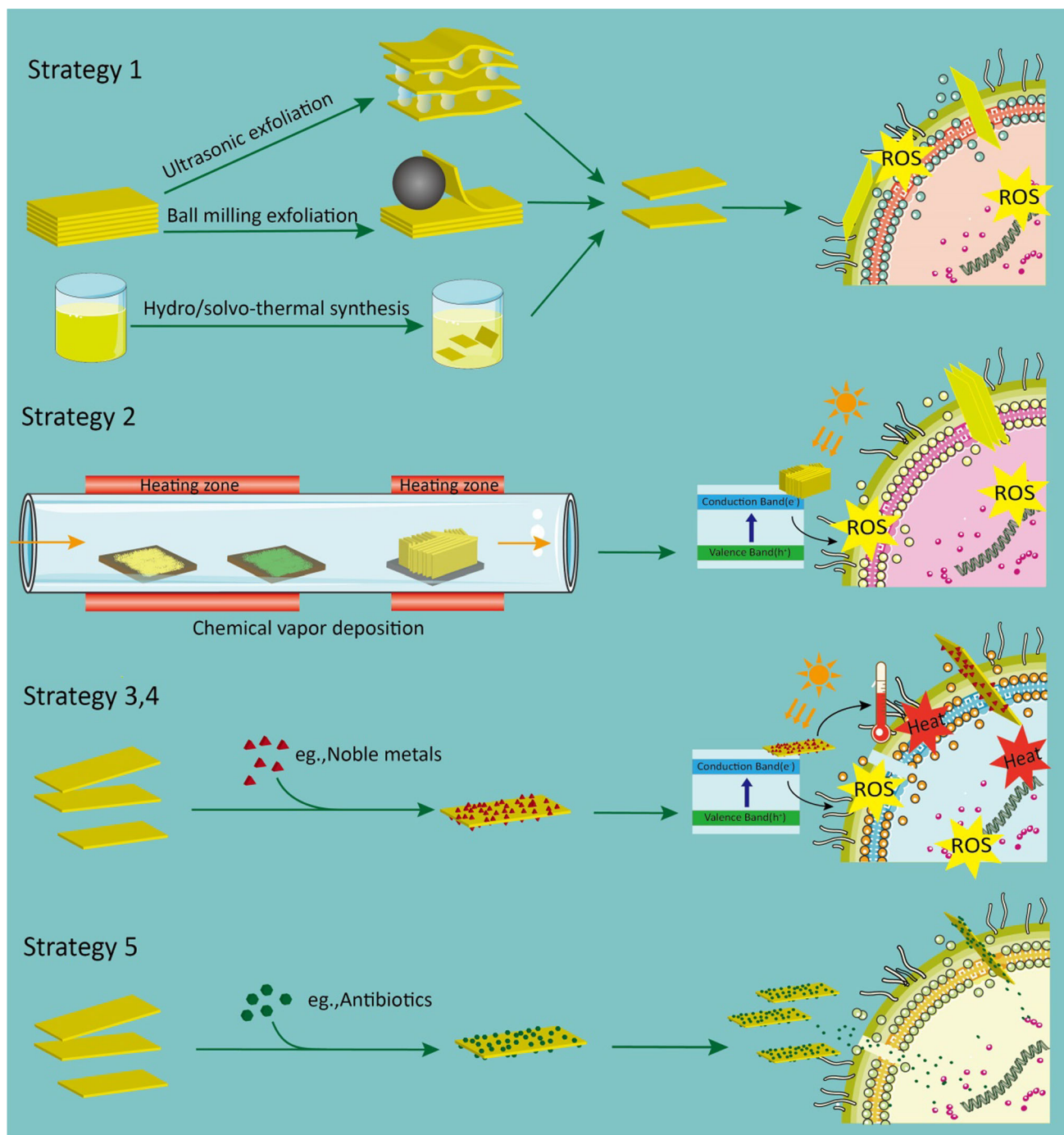
Figure 2 Schematic illustration of how the different strategies enhance the antimicrobial activities of pg-2DMs-AA. Strategy 1: fabricating single- or few-layer pg-2DMs; strategy 2: building vertical structures; strategies 3 and 4: decorating with other materials to enhance the photocatalytic and/or photothermal activity; strategy 5: loading with other antibacterial agents.

(PCE), all of which can induce membrane and oxidative stress to microbes [19]. For some pg-2DMs, such as MoS_2 and $MoSe_2$, decreasing their layer numbers will also change their band gaps from indirect to direct band gaps [20, 21], which results in the increase in their photocatalytic and/or photothermal activities, and thereby improve their antimicrobial efficiencies. Now, the common approaches to prepare single- or few-layer pg-2DMs for antimicrobial applications include the top-down
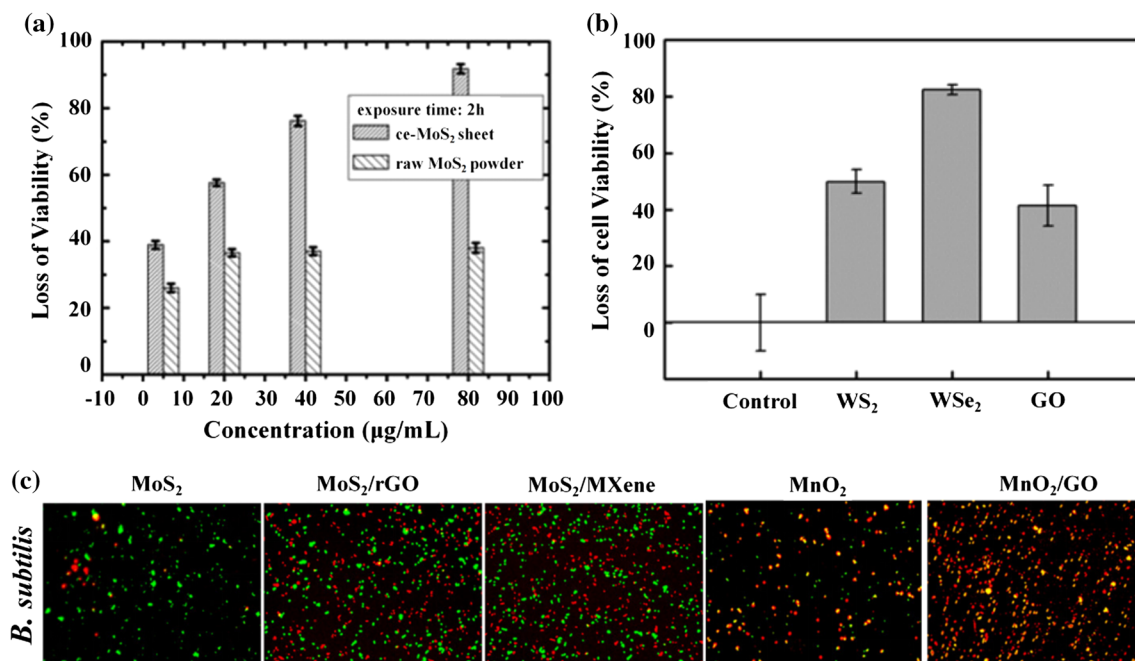
Figure 3 **a** Viabilities of the *E. coli* DH5a incubated with different concentrations (5–80 µg/mL) of ce-MoS$_2$ sheets or raw MoS$_2$ powders for 2 h. Reproduced with permission from Ref. [19]. Copyright 2014, Royal Society of Chemistry. **b** Antibacterial properties of WX$_2$-ssDNA and GO nanosheets. (The viabilities of *E. coli* cells decreased when they were treated with 80 µg/mL WX$_2$-ssDNA or GO nanosheets for 5 h.) Reproduced with permission from Ref. [34]. Copyright 2016, American Chemical Society. **c** Fluorescence images of *B. subtilis* that were treated with 100 µg/mL MoS$_2$, MoS$_2$/rGO, MoS$_2$/MXene, MnO$_2$ and MnO$_2$/GO nanomaterials for 3 h in dark. Red and green dots represented the live and dead bacteria, respectively. Reproduced with permission from Ref. [46]. Copyright 2018, American Chemical Society.

exfoliation method (e.g., ball milling exfoliation, liquid-based ultrasonic exfoliation) and the down-top method (e.g., hydro/solvo-thermal synthesis) (Fig. 2).

Ball milling exfoliation

The micromechanical cleavage technique is the traditional mechanical exfoliation method utilized to cleave thin graphene flakes from their parent bulk crystals by the scotch tape [22]. The method was soon applied in other 2D materials such as MoS$_2$ and WSe$_2$ [23]. However, this method is low yield and the thickness, size and shape of the resultant materials are difficult to control as this method is mainly operated by hands. Obviously, this method is for fundamental researches but not suitable for antimicrobial applications that need convenient and scalable productions of thin-layer 2D materials. To overcome this drawback, the method of ball milling, generating two types of force-shear force and compression force, has garnered attentions. For instance, Feng et al. mixed bulk MoS$_2$ with chitosan and ionic liquid, which were ground in a planet ball mill afterward. After the grinding process, the mixture was collected and washed with acetone, *N*, *N*-dimethylformamide and 0.5% acetic for three times to remove the ionic liquid and the excess chitosan. Chitosan improved the dispersibility and stability of MoS$_2$ and increased the thickness of the resultant MoS$_2$ nanosheets (approximately 4.7 nm). This chitosan-modified MoS$_2$ nanosheets inactivated *E. coli* and *Staphylococcus aureus* significantly [24]. Zhang et al. [25] exfoliated bulk MoS$_2$ with the assistance of ionic liquid using a similar mechanical method, in which the authors used an agate mortar and a pestle to grind the mixture instead of the planet ball mill.

Liquid-based ultrasonic exfoliation methods

Ultrasonication is frequently used to exfoliate 2D materials as well. When the ultrasonic waves propagate through the medium, the interaction between the ultrasonic waves and the medium causes physicochemical changes, resulting in a series of chemical, thermal, electromagnetic and mechanical

ultrasonic effects. The cavitation in the liquid is the main cause of exfoliation. When the cavitation bubble explodes, microjets and shock waves are generated, which lead to the erosion and structural damages on the material surfaces, as well as the exfoliation and collision between the material particles [26]. Yet, using ultrasonication to directly exfoliate 2D materials can hardly be accomplished in water unless some appropriate additives or stabilizers are supplemented, due to the strong hydrophobic characters of many 2D materials [27]. Organic solvents (e.g., isopropyl alcohol [28], dimethylformamide [29] and sodium cholate [30]) with appropriate surface tensions to match the surface energy of the targeted 2D material well, are often chosen because of their important roles in reducing the potential energy barriers that exist in the interlayers of bulk 2D materials and in the stabilization of resultant nanosheets by interfacial interactions [27]. Adding intercalants such as Li ions also improves the exfoliation of bulk 2D materials [19], because the insertion enlarges the interlayer spacings of bulk 2D materials and then weakens the interlayer interactions, and finally facilitates the subsequent ultrasonic exfoliation [27].

The aforementioned methods have the advantages of high yield and large scale, and the products also show good antibacterial activities. But some solvents, such as N-methyl-2-pyrrolidone and N-cyclohexyl-2-pyrrolidone, may adsorb on the resultant nanosheets and are difficult to be removed completely [31]. This is not conducive for the wider biomedical applications of the resultant materials. In addition, most of the used surfactants are synthetic, which will raise the concerns about the cost, environmental impact and biocompatibility of the resultant 2D materials [32]. Meanwhile, the alkali metal intercalation-assisted exfoliation is time-consuming (about several days) and the used organometallic materials are highly explosive and sensitive to the moisture and oxygen, which needs strict experimental conditions with extreme cautions [33]. To overcome these limitations, researchers pay attentions to the biomolecules (e.g., nucleic acids, proteins, polysaccharides) in recent years, as they can serve as the more sustainable and environment-friendly natural stabilizers for 2D materials [32]. Until now, nucleic acids [34], proteins [35] and chitosan [36] have been utilized successfully. For instance, Bang et al. have reported an

effective and high-yield exfoliation technique for WS_2 and WSe_2 under aqueous conditions with the assistance of ssDNA. The nonpolar nucleobase of ssDNA can readily adsorb onto the surface of WS_2 and WSe_2, whereas the polar phosphate group is able to extend into and strongly interact with the aqueous medium, furnishing the resultant materials with colloidal stability due to the steric and electrostatic repulsion. Interestingly, the as-prepared WS_2 and WSe_2 nanosheets showed higher antibacterial activities against E. coli than that of graphene oxide (Fig. 3b) [34]. Silk fibroin also has an amphiphilic structure and hydrophilic/hydrophobic multi-block domains and thereby can be used for the exfoliation and stabilization of 2D materials. Huang et al. exfoliated bulk $MoSe_2$ with the assistance of carboxyl-modified silk fibroin (CMSF). The authors report that the resultant $MoSe_2$/CMSF nanosheets own peroxidase-like activity and can turn low concentrations of H_2O_2 into ROS to kill E. coli and Bacillus subtilis [35].

However, in all the above cases, exfoliated 2D materials are not covalently functionalized, which causes instability over time and limit their applications. Recently, Chou and coworkers have reported that chemically exfoliated MoS_2 nanosheets with defects in both internal edges and perimeter edges are amenable to the thiol ligand modifications [37]. Similarly, Pandit et al. exfoliated MoS_2 using the lithium intercalation-assisted sonication method. Then to functionalize the surface of the material, they mixed the exfoliated MoS_2 nanosheets with different thiol ligand solutions. They found that the functionalized MoS_2 nanosheets showed higher stability in aqueous media and the positively charged MoS_2 nanosheets inactivated methicillin-resistant S. aureus and Pseudomonas aeruginosa effectively at very low concentrations (156 ppb and 78 ppb, respectively) [38]. This thiol ligand-based functionalization method is further optimized by Karunakaran et al. [39]. They synthesized surfactant thiol ligands with amphiphilic properties, by which they efficiently exfoliated and functionalized 2H-MoS_2 simultaneously in aqueous medium without the assistance of lithium intercalation. The functionalized MoS_2 nanosheets showed perfect bactericidal effects. All these works demonstrate the possibilities of fabricating pg-2DMs-AA with long-lasting stabilities by the covalent functionalization method.

Hydro-/solvo-thermal synthesis

The hydro- or solvo-thermal synthesis method, belonging to the down-top approaches, relies on the suitable "metal–organic" molecules as the precursors for the direct synthesis of the few-layer 2D materials in the solution [40]. The solvent contains the polymer or surfactant, and the precursor is kept in sealed vessels or autoclaves and heated over its boiling point. This process will promote the reduction of the precursor salts into 2D sheets. Because of large-scale production, easy and inexpensive synthesis of nanostructured materials, hydro-/solvo-thermal synthesis methods have been frequently used to attain few-layer 2D materials with interesting structures and sometimes the doping of foreign nanomaterials, which can endow excellent antimicrobial activities to the as-prepared materials. For instance, Cao et al. synthesized PEG-MoS_2 nanosheets using a modified solvo-thermal method. In short, 60 mg thioacetamide (C_2H_5NS) and 30 mg sodium molybdate ($Na_2MoO_4 \cdot 2H_2O$) were dissolved in 20 mL PEG-200 aqueous solution (50%, v/v) and then transferred into a 100-mL polyphenylene-lined stainless steel autoclave, which was heated at 200 °C for 24 h afterward. The resultant MoS_2-PEG nanosheets were further decorated with L-cysteine, silver ion and the cationic polyelectrolyte to obtain the PDDA-Ag^+-Cys-MoS_2 nanocomposites. This nanocomposite exhibited perfect broad-spectrum antibacterial activities due to its high accessibility of released Ag^+ to the bacterial cell wall [41].

Building vertical structures

Past studies have shown that vertical graphene can kill bacteria via membrane destroy and ROS damage [42–44]. For instance, Lu and coworkers found that the antibacterial activity of graphene oxide was related to its orientation. Among the vertical, random and planar graphene oxide (GO), vertical structure exhibited the highest antibacterial activity against *E. coli*. The cell mortality of vertical GO ($44.0 \pm 8.7\%$) was 1.5 times higher than that of the random ($25.7 \pm 3.5\%$) and twice of the planer ($19.2 \pm 5.1\%$) [43]. Similar to graphene, MoS_2 with vertical structures exhibits excellent bactericidal activity as well. For example, Liu et al. prepared the few-layered vertically aligned MoS_2 (FLV-MoS_2) by a chemical vapor deposition (CVD) technique. Under the visible light, FLV-MoS_2 showed > 99.999% *E. coli* inactivation in 120 min. FLV-MoS_2 in the dark showed < 50% disinfection efficiency after 120 min, and bulk MoS_2 just showed a 54% efficiency over 120 min. The authors conclude that FLV-MoS_2 owns a higher in-plane electrical conductivity and catalytic activity on the edge sites. Thus, FLV-MoS_2 has a better electron–hole transport from MoS_2 to the electrolytes and so exhibits a better photocatalytic activity, which increases the ROS generation and the subsequent bactericidal activity [45]. The vertically aligned MoS_2 structure also has more sharp edges, which will destroy bacterial cell walls and reduce membrane integrity more efficiently [46]. The vertically aligned MoS_2 structure can be decorated with other materials to further boost its antibacterial activity. Liu et al. obtained a uniform, dense and nearly vertical growth of MoS_2 on the conductive support-polyaniline nanorods by a hydrothermal method [47]. These MoS_2-polyaniline nanorods have large amount of active edges and perfect electron transfer efficiency, resulting in the excellent photocatalytic activity. After 3 h of visible light irradiation, the MoS_2-polyaniline nanorods almost completely kill *E. coli*. Tang et al. vertically coated MoS_2 nanosheets (with or without the doping of iron) on the titanium substrate via a one-step hydrothermal reaction. The resultant MoS_2 hybrids showed satisfying antibacterial activities without the irradiation of visible light. The authors suggested that the doping of iron enhanced the bactericidal activities by releasing ferrous ions and boosting the ROS generation via Fenton-like reactions [48]. Alimohammadi et al. investigated the antimicrobial properties of the randomly oriented MnO_2, MoS_2 and vertically aligned MnO_2/GO, MoS_2/rGO, MoS_2/MXene. As shown in Fig. 3c, the percentages of viable *B. subtilis* bacteria decreased from 95 to 60% (MoS_2/rGO) and to 75% (MoS_2/MXene). The vertically aligned MnO_2/GO showed a remarkable bactericidal activity as the percentage of the viable bacteria decreased to 10% [46].

Due to the advances of synthetic methods, the range of vertical 2D materials has extended to other 2D materials, including TMDs [45, 49–51], h-BN [52], MoO_3 [53], g-C_3N_4 [54], MXene [55] and layered double hydroxide [56, 57]. However, the vertical aligned form of other 2D materials except graphene, MnO_2 and MoS_2 is still scarcely investigated for bactericidal applications.

Decorating with other materials to enhance the photocatalytic activity

Photocatalysis will be initiated when the photocatalyst surface is bombarded by photons with enough energy. Irradiation of light with suitable wavelength (> the band gap of the photocatalyst) activates the electrons (e^-) to escape from the valence band of the photocatalyst. When the e^- leaves and is absorbed onto the conduction band (e^-_{CB}), a positive hole is formed on the valence band (h^+_{VB}) [58]. e^-_{CB} and h^+_{VB} lead to the formation of reactive species such as superoxide radicals, hydroperoxide radicals and hydroxyl radicals, which cause the microbe inactivation [59]. Therefore, the electron (e^-)/hole (h^+) separation and transportation to the photocatalyst surface are critical for the generation of reactive species and the following antimicrobial efficiencies.

One way to modulate the separation and transportation of e^-/h^+ is fabricating specific morphologies (e.g., zero-dimensional (0D) structure [60], vertically aligned structure [45], microflower structure [61]) to change the microbe inactivation effects. Another common way is to couple with foreign materials to form heterostructures, which will be discussed in this section. It has long been known that the photocatalytic performance of the single-component photocatalyst is not ideal due to the high recombination rate of photo-generated electrons and holes. Combining one photocatalyst with other materials to form the heterostructures facilitates the charge transfer between the different photocatalysts and promotes the separation of charge carriers [62, 63]. Among pg-2DMs, graphitic carbon nitride (g-C$_3$N$_4$) is a popular star in photocatalytic infection applications due to its broad light response spectrum (up to 460 nm), high stability and ease being fabricated and tuned to various morphologies. Yet, pristine g-C$_3$N$_4$ shows limited photocatalytic efficiency because of the high recombination rate of photo-generated charges and low surface area [64]. To overcome this drawback, other materials (e.g., graphene and its derivatives, noble metals) that serve as the electron sink, conductive mediator, photosensitizer and absorbent, are selected to couple with g-C$_3$N$_4$ and the resultant heterostructures show perfect microbial inactivation abilities. (This has been summarized by Liu et al. [65].) Apart from g-C$_3$N$_4$, MoS$_2$ also gets increasing attentions in the photocatalysis area [66]. MoS$_2$ is a semiconductor material with a narrow band gap ($\sim$ 1.8 eV) because it has a strong absorption in the visible region of solar spectrum [67]. But the fast recombination of photo-generated charges and reduced conductivity of MoS$_2$ confine its application as the cocatalyst [68]. If it is attached with other materials such as graphene [69] and carbon [70], however, it turns out to be an efficient cocatalyst. For instance, graphene supports to improve the photocatalytic performance of MoS$_2$ by acting as an excellent electron acceptor and transporter. Compositing MoS$_2$ with reduced graphene (rGO) is a low-cost and efficient alternative for improving the photocatalytic activity of MoS$_2$. The synergetic effect between MoS$_2$ and rGO can be further boosted by the doping of ZnO, and the resultant composites display excellent photocatalytic and antibacterial activities [61]. Wang et al. combined the hydrothermal carbonation carbon (HTCC) with MoS$_2$ to form the HTCC@MoS$_2$ heterojunction. Compared with the single-component HTCC and MoS$_2$, the binary composites HTCC@MoS$_2$ exhibited super-bactericidal capacities because of their excellent photocatalytic activities (Fig. 4a) [70].

Decorating with other materials to enhance the photothermal activity

Photothermal bacterial inactivation refers to hyperthermia damage to the bacterial cells using the combination of photothermal agents and light. The agents absorb the light and transfer the energy into heat through nonradiative relaxation, which will cause irreparable damage to the bacterial cells nearby [71]. For example, Miao et al. found that two-dimensional Sb$_2$Se$_3$ nanosheets exhibited perfect optical absorbance from the ultraviolet to the NIR region, and thus owned excellent photothermal performances. The temperature change of 300 μM Sb$_2$Se$_3$ nanosheets suspensions reached 29.9 °C when it was irradiated with a laser power (808 nm, 2 W). After being treated with 300 μM Sb$_2$Se$_3$ nanosheets under the irradiation for 5 min, the viabilities of *E. coli* and methicillin-resistant *S. aureus* (MRSA) all decreased to 0% (Fig. 4b) [72].

Some pg-2DMs (e.g., MoS$_2$, MXenes) can be served as excellent photoabsorbing agents. Decorating with other materials can further enhance their photothermal infection performances [73, 74]. In this regard, because of their surface plasmon resonance
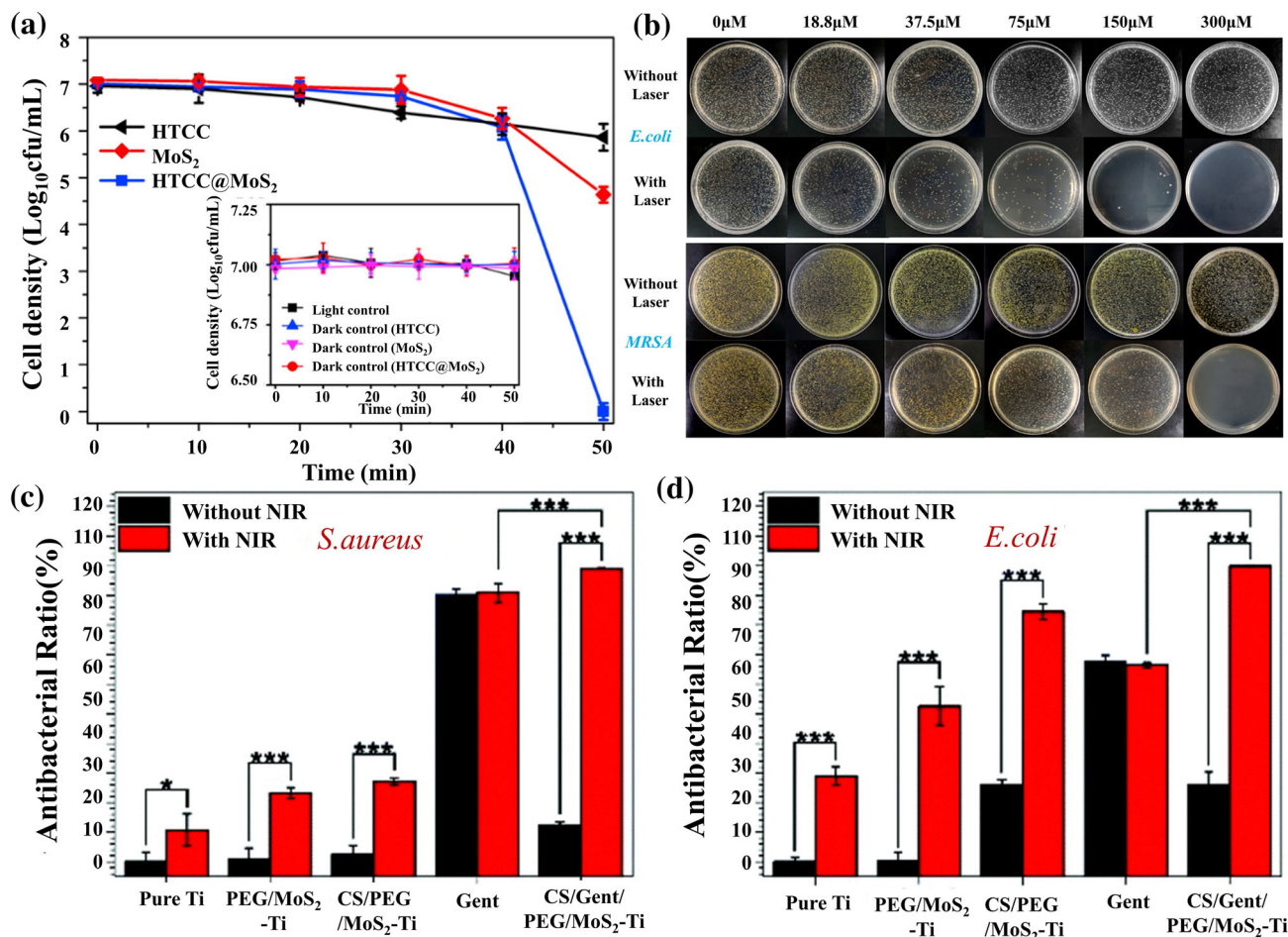
Figure 4 **a** Cell density of *E. coli* K-12 treated with 1 mg/mL HTCC, MoS$_2$ and HTCC@MoS$_2$ at 37 °C for 18 h in light. (Inset represents the light and dark controls.) Reproduced with permission from Ref. [70]. Copyright 2019, ELSEVIER. **b** Pictures of *E. coli* and *MRSA* colony formation in the presence of Sb$_2$Se$_3$ nanosheets with or without the laser irradiation (808 nm, 2 W) for 5 min and followed by incubation for 24 h and 48 h. Reproduced with permission from Ref. [72]. Copyright 2019, American Chemical Society. **c, d** The activities of *S. aureus* (**c**) and *E. coli* (**d**) on pure Ti, PEG/MoS$_2$–Ti, CS/PEG/MoS$_2$–Ti, Gent and CS/Gent/PEG/MoS$_2$–Ti without or with NIR irradiation for 5 min. The error bar indicates means ± standard deviations (n = 3): *p < 0.05, ***p < 0.001. Reproduced with permission from Ref. [78]. Copyright 2019, Royal Society of Chemistry.

absorption abilities, noble metals, such as gold and silver [75], are often selected to decorate pg-2DMs to achieve better photothermal conversion efficiencies (PCE). For instance, Lin et al. fabricated a kind of Ag$_2$S@WS$_2$ heterostructure, which exhibited strong optical absorption and high photothermal conversion efficiency. They found that pure WS$_2$ and Ag$_2$S@WS$_2$ heterostructure can reach 30 °C and 60 °C, respectively, under the irradiation of NIR (808 nm) for 10 min. Pure WS$_2$ showed a very weak antibacterial ability. In contrast, the antibacterial efficacy of Ag$_2$S@WS$_2$ reached up to 99.93% and 99.84% against *S. aureus* and *E. coli*, respectively [76]. Besides, in comparison with bare black phosphorus (BP) nanosheets, gold nanoparticle-decorated BP nanosheets showed 8% increase in PCE, caused by the surface-enhanced Raman scattering (SERS) of gold nanoparticles [77]. Zhang et al. decorated MoS$_2$ nanosheets with Fe$_3$O$_4$ nanoparticles, which aggregated the MoS$_2$ nanosheets and thus increase the local heat around MoS$_2$ nanosheets during the near-infrared (NIR) irradiation, finally leading to better antibacterial activities [25].

Loading with other antibacterial agents

Pg-2DMs have large specific surface areas, making them to be perfect platforms to load small molecular antibacterial agents. Zhang et al. successfully loaded tetracycline hydrochloride drugs into the chitosan-functionalized MoS_2 nanosheets. In terms of the antibacterial and antibiofilm activities, the combination of MoS_2 nanosheets and antibiotics was more efficient than either working alone [7]. Moreover, the release of the loaded antibiotics can be controlled to achieve better antimicrobial efficiencies by the photothermal properties of some pg-2DMs. Ma et al. developed a photothermally modulated drug release system on the implant surface for in situ rapid disinfection. This system, called CS/Gent/PEG/MoS_2–Ti, consists of chitosan (CS), gentamicin (Gent), polyethylene glycol (PEG), MoS_2 and a titanium implant. When the CS/Gent/PEG/MoS_2–Ti system is under the radiation of NIR, the photothermal component MoS_2 increases the temperature and thus accelerates the release of Gent. Meanwhile, hyperthermia weakens the bacterial activity and enhances the membrane permeability, which helps the drugs to penetrate into the bacteria. When maintained at 50 °C for 5 min under NIR irradiation, this system can achieve infection efficiencies of 99.93% and 99.19% against *E. coli* and *S. aureus*, respectively. In contrast, even treated for 120 min by Gent alone, only a 93.79% antibacterial ratio can be obtained (Fig. 4c, d) [78].

In addition to MoS_2, LDHs are often utilized as the carriers of antibacterial agents as well. The interlayer space of LDHs can be intercalated with different ions. In addition, they have good biodegradability, composition-dependent properties and are easy to be prepared, all of which make LDHs become the ideal reservoirs for sustained and controlled drug release. Thus far, numerous antibacterial agents (e.g., antibiotics [79, 80], DL-mandelic acid [81], silver nanoparticles [82], lysozyme [11, 83]) have been loaded into LDHs. (More information can be found the review contributed by Sun et al. [6].)

As the candidates for preparing novel bactericidal materials, many pg-2DMs provide new solutions to the increasingly serious bacterial infection problem. To fuel the development of this field, we would like to point out some interesting directions for the future research:

(1) Since many pg-2DMs own large specific surface areas and lysozyme has been successfully loaded onto LDHs [11], it might be possible to fabricate more efficient and less toxic antimicrobial agents by combining the antimicrobial peptide with some suitable pg-2DMs.

(2) Recent findings demonstrate that the phase of MoS_2 can be controlled by tuning the synthesis conditions [84, 85]. Interestingly, MoS_2 in 1T phase shows higher catalytic activities [86, 87], which might be utilized to generate more ROS for antimicrobial purposes. Therefore, using the methods in phase engineer to synthesize some pg-2DMs with specific phases and simultaneously decorating with foreign materials such as noble metal and metal oxides may obtain fancy antimicrobial nanocomposites.

Biosafety assessment of post-graphene 2D materials-based antimicrobial agents

While recognizing the advantages and potential huge markets of pg-2DMs in antibacterial fields, a scientific and social issue has also caught the attention of researchers—the biosafety of these pg-2DMs-AA. Biosafety, referring to the risks to the human health and environment, is the primary importance for choosing materials that are valuable to the fields like biomedicine. The biosafety of the pg-2DMs-AA being intended to be applied in the biomedicine or public health must be thoroughly evaluated prior to their practical applications. The hazard potentials of pg-2DMs themselves are not within the scope of this review because they have already been summarized by some recently published reviews [88, 89]. Here, we summarized the biosafety assessments of the antimicrobial agents fabricated by pg-2DMs or their derivatives. As shown in Fig. 5a, some researchers evaluate the biosafety of the resultant pg-2DMs-AA via in vitro assessment and/or in vivo assessment. Only a few of them explore the environmental risks of pg-2DMs-AA. Most of the prepared pg-2DMs-AA (around 70.32%) are not received any biosafety assessment. So far, the biosafety of pg-2DMs-AA fabricated by MoS_2 is studied most intensively (Fig. 5b).
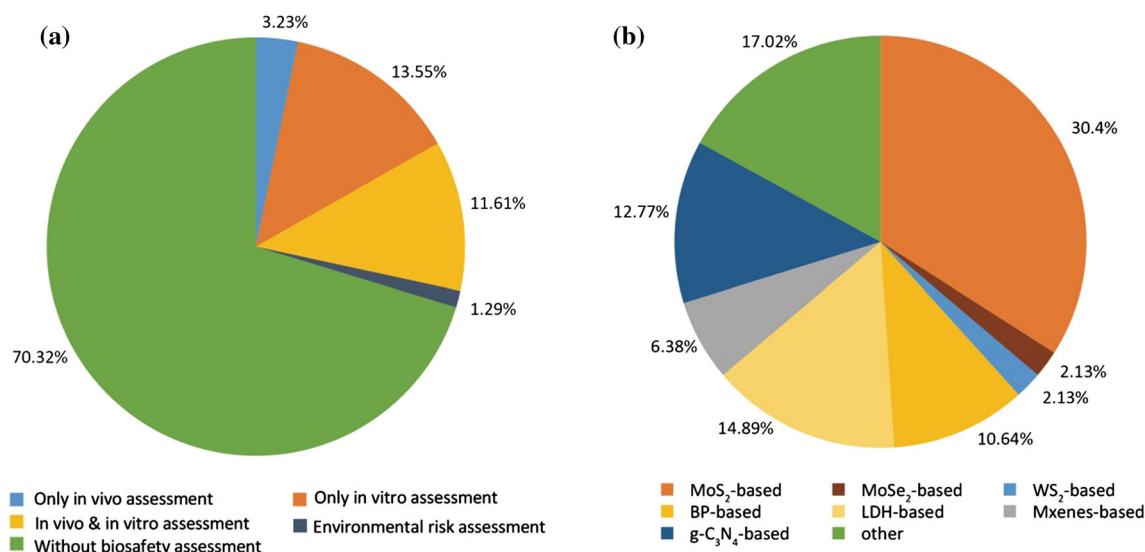
Figure 5 **a** Percentage of the pg-2DMs-AA-associated publications with or without biosafety assessment; **b** percentage of different pg-2DMs-based antimicrobial agents whose biosafety has been assessed.

Assessing the risks to human health

In vitro assessment

In vitro assessment is generally performed by cell cultures, which are used as prescreening tools to unveil the toxicities of bactericidal nanomaterials and the mechanisms of action [4]. The selected cells include tumor cells (e.g., HeLa cell [8, 10, 90, 91], hepatoma cell [25], MDA-MB-231 cell (human breast cancer cell) [10, 92], KU-7 cell (urothelial carcinoma cell line) [93]) and normal cells derived from different tissues (e.g., HUVEC cell (human umbilical vein endothelial cell) [91], buffalo rat liver 3A cell [25], erythrocyte [39, 94], fibroblast cell [10, 95], human mesenchymal stem cell [10]). As summarized in Table 1, the cytotoxicities of these antimicrobial agents are often tested by colorimetric assays, which determine the variations of cell viability and proliferation (such as MTT and CCK-8 assay), and cell membrane stability (such as lactate dehydrogenase and hemolysis assay). In addition to the colorimetric assays, qRT-PCR is also utilized to detect the impacts of these pg-2DMs-AA on the gene expressions. For instance, Mao et al. have prepared a kind of black phosphorus (BP) nanosheets chitosan hydrogel to promote bacteria-accompanied wound healing. MTT assay indicates that the BP hydrogel enhances the viability of NIH-3T3 cell. The authors further investigate the expressions of smooth muscle α-actin

(α-actin) and type III collagen (COL III) gene. They find the BP hydrogel facilitates the expressions of these two genes, suggesting the BP hydrogel facilitates the fibroblast cells to differentiate into myofibroblasts, and the tissue reorganization and basement membrane regeneration (Fig. 6a–d) [96].

In vivo assessment

Bactericidal nanomaterials can penetrate into human body by the skin exposure or inhalation and then influence the major organs like lung, heart and brain. The in vivo toxicological effects of bactericidal nanomaterials are much more complicate than their in vitro effects, because the circumstances within the body are more complex than those in the cell culture medium. Thus, the results from the cell culture studies need to be confirmed by in vivo studies. Currently, in vivo assessments for pg-2DMs-AA are conducted by analyzing the histological structures of the major organs [8, 10, 31, 41, 96, 97] and/or measuring body weights of the tested animals [91, 97] (Table 1). For example, Shao et al. fabricated a kind of thermosensitive hydrogel containing black phosphorus nanosheets (BP@PLEL hydrogel). The hydrogel was subcutaneously injected into the rear parts of the Balb/c mice (6 weeks old). The mice were killed 20 days after the injection, and their major organs (liver, spleen, kidney, heart and lung) were collected and then analyzed by H&E staining. No apparent

Table 1 Biosafety assessment of the post-graphene 2D materials-based antimicrobial agents

Aim	Components	Cells or organisms	Method and concentration	Main findings	Reference
Health risk assessment	Chemically exfoliated MoS_2 (ce-MoS_2) functionalized by thiol ligands	HeLa cell	MTT assay (6.28–8320 µg/mL)	Functionalized ce-MoS_2 exhibited very low cellular toxicity	Ref. [90]
	Polyethylene glycol-functionalized molybdenum disulfide nanoflowers (PEG-MoS_2)	HeLa cell HUVEC cell Four-week-old Kunming mice	Cell counting kit-8 (CCK-8) assay (0, 10, 25, 50, 100 and 250 µg/mL) Body weight measurement (15 mg/kg)	After being incubated for 24 h, the viability of HeLa cells > 90% (HUVEC cells > 85%) even in the concentration up to 250 µg/mL Similar to the control, the body weight of the mice injected with PEG-MoS_2 increased gradually in 30 days	Ref. [91]
	Chitosan-functionalized MoS_2 decorated with Fe_3O_4 nanoparticle	Human hepatoma cell Mouse microglia cell Buffalo rat liver 3A cell	MTT assay (10, 20, 50, 100, 200 µg/mL)	> 80% of the incubated cells remained viable in all the applied concentrations	Ref. [25]
	PDDA-Ag^+-Cys-MoS_2	Mice	Immunohistochemistry test (H&E staining) (15, 50 µg/mL)	No appreciable abnormalities or damages were observed in the major organs 3 days after PDDA-Ag^+-Cys-MoS_2 injection	Ref. [41]
	MoS_2–TiO_2 nanocomposites	Erythrocyte	Hemolysis assay (25, 500, 1000 µg/mL)	Stability of the erythrocyte membrane was not damaged	Ref. [94]
	Chitosan-functionalized MoS_2 nanosheets loading tetracycline hydrochloride drugs	Human hepatoma cell Mouse microglia cell	MTT assay (56.4–902.4 µg/mL)	Cell viability > 90% when the exposure concentration was 225.6 µg/mL	Ref. [7]
	Thiolated ligand-functionalized exfoliated 2H MoS_2	Rabbit erythrocyte	Hemolysis assay (9.45–4752 µg/mL)	2H-MoS_2 functionalized with the thiolated ligands exhibits minimal lysis to erythrocytes (no more than 5%)	Ref. [39]
	MoS_2 nanosheets modified with polydopamine and silver nanoparticles (MPA NSs)	HeLa cell Balb/c mice (6 weeks old)	Lactate dehydrogenase assay (10, 20, 40, 80, 160, 320 µg/mL) Histological analysis (H&E staining) (5 mg/kg)	Cell viability was not changed at the concentration up to 320 µg/mL. No noticeable damages or inflammatory lesions were found in the major organs (heart, liver, spleen, lung and kidney)	Ref. [8]

Table 1 Biosafety assessment of the post-graphene 2D materials-based antimicrobial agents

| Aim	Components	Cells or organisms	Method and concentration	Main findings	Reference
	MoS_2 modified with chitosan and silver nanoparticle	Nude mice (6 week old)	Histological analysis (H&E staining) (2 mg/kg) Body weight measurement (2 mg/kg)	No obvious weight variation compared with the control No significant effects on the organs	Ref. [97]
	Black phosphorus nanosheets-chitosan hydrogel	NIH-3T3 cell Male Wistar rats	MTT assay qRT-PCR immunohistochemistry test	Enhanced the cell viability and the gene expressions of COL III and α-actin After 14 days of treatment. No appreciable abnormalities or damage was found in the major organs	Ref. [96]
	Black phosphorus nanosheet-incorporated poly(d,l-lactide)-poly(ethyleneglycol)-poly(d,l-lactide) hydrogel (BP@PLEL)	Human mesenchymal stem cell Mouse fibroblast cell Human breast cancer cell HeLa cell Mice (6 weeks old)	CCK-8 assay (150 μL of the medium containing BP@PLEL hydrogel (50 ppm BP and 30% (w/v) hydrogel) Immunohistochemistry test (200 μL aliquots of 30% (w/v) BP@PLEL hydrogel with 50 ppm BP)	No significant cytotoxicity No apparent histological abnormality or lesion was found in liver, spleen, kidney, heart and lung	Ref. [10]
	Black phosphorus nanosheets poly (4-pyridonemethylstyrene) endoperoxide film	Mice	Immunohistochemistry test	No signals of abnormalities or lesions were found in liver, spleen, kidney, heart and lung	Ref. [31]
	Au/g-C_3N_4 hybrid	NIH3T3 and MDA-MB-231 cells	MTT assay (0, 2, 50, 100, 200 μg/mL)	No noticeable cell toxicity was uncovered	Ref. [92]
	Layered double hydroxides (LDH)-silver nanoparticle (AgNP) hybrids	Lung fibroblast cell line	MTT assay (0, 20, 30, 40, 45, 50 μmol/mL)	LDH-AgNP hybrids and pure LDH did not exhibit cytotoxicity at the concentration up to 50 μmol/L. LDH alleviated the toxicity of AgNP	Ref. [95]
	Layered double hydroxide (LDH) clays binding different antibiotics (tetracycline, doxorubicin, 5-fluorouracil, vancomycin, sodium fusidate and antisense oligonucleotides)	KU-7 cell	MTT assay (0.03, 0.06, 1, 2, 10 mg/mL) Lactate dehydrogenase assay (0.03, 0.06, 1, 2, 10 mg/mL)	Cell viability was reduced by LDH clay, but it remained high (> 70%). No significant difference in cell viability when LDH clay concentrations < 10 mg/mL LDH clay produced only minor damage to the cell membrane stability (< 10% of positive control)	Ref. [93]

Table 1 continued

Aim	Components	Cells or organisms	Method and concentration	Main findings	Reference
Environmental risk assessment	Ti_3C_2 MXene, $Ti_3C_2/Al_2O_3/Ag$, $Ti_3C_2/SiO_2/Ag$ and $Ti_3C_2/SiO_2/Pd$ nanocomposites	Green algae (*Desmodesmus quadricauda*) Sorghum (*Sorghum saccharatum*) Charlock (*Sinapis alba*)	Algal growth assessment (12.5–100 mg/L) Phytotoxicity analysis (germination, root growth) (100, 200 mg/kg of soil)	The prepared nanocomposites caused both stimulating and inhibiting effects toward algae Pristine Ti_3C_2 stimulated the growth of green algae at low concentrations. Modifying pristine Ti_3C_2 MXene with different nanoparticles changed the ecotoxicities of the resultant nanocomposites	Ref. [102]
	Ti_3C_2Tx (MXene)	Zebrafish embryo	Acute toxicity assay (25, 50, 100 and 200 μg/mL) Locomotion and neurotoxicity assays (50 μg/mL)	LC50 of Ti_3C_2Tx was 257.46 μg/mL, and the highest NOEC (< 20% mortality) was 50 μg/mL. No significant teratogenic effects were observed on zebrafish embryos at 100 μg/mL. The results of locomotion and neurotoxicity assays indicated that 50 μg/mL Ti_3C_2Tx did not damage the neuromuscular activities	Ref. [101]

histological abnormality or lesion was observed in the mice treated with the BP@PLEL hydrogel, suggesting the hydrogel was safe within the body (Fig. 6e) [10].

Assessing the risks to environment

Nanomaterial-based antimicrobial agents widely used in human medicine, water infection or food packing will inevitably be released into the environment. They can have deleterious effects on sensitive organisms, especially the wild microorganisms, which may cause disorders in the ecosystem. Therefore, the potential impact of antimicrobial agents on the ecosystem must be evaluated as closely as other hazardous chemicals [98]. So far, the ecotoxicities of nanomaterial-based antimicrobial agents (e.g., quantum dots based [99], ZnO nanoparticle based [100]) have been explored.

However, the studies exploring the ecotoxicities of pg-2DMs-AA are still in infancy. Only two studies are found and introduced here. For instance, after exploring the antibacterial activity of Ti_3C_2Tx (MXene), Khaled A. Mahmoud's group further investigated the ecotoxicity of Ti_3C_2Tx by evaluating its impacts on zebrafish embryos and the motor and nervous system of zebrafish larvae (Fig. 7a) [13, 101]. They found that the LC50 of Ti_3C_2Tx was 257.46 μg/mL. No significant teratogenic effects were observed on zebrafish embryos at 100 μg/mL. Locomotion and neurotoxicity assays further supported the nontoxicity of Ti_3C_2Tx at a concentration of 50 μg/mL. Rozmysłowska et al. examined how the modifications of the antimicrobial Ti_3C_2 MXene with ceramic oxide and noble metal nanoparticles affect the corresponding ecotoxicities. Three nanocomposites ($Ti_3C_2/3\%$ $Al_2O_3/2\%$ Ag, $Ti_3C_2/3\%$ $SiO_2/2\%$ Ag and $Ti_3C_2/3\%$ $SiO_2/2\%$ Pd) were synthesized, and their
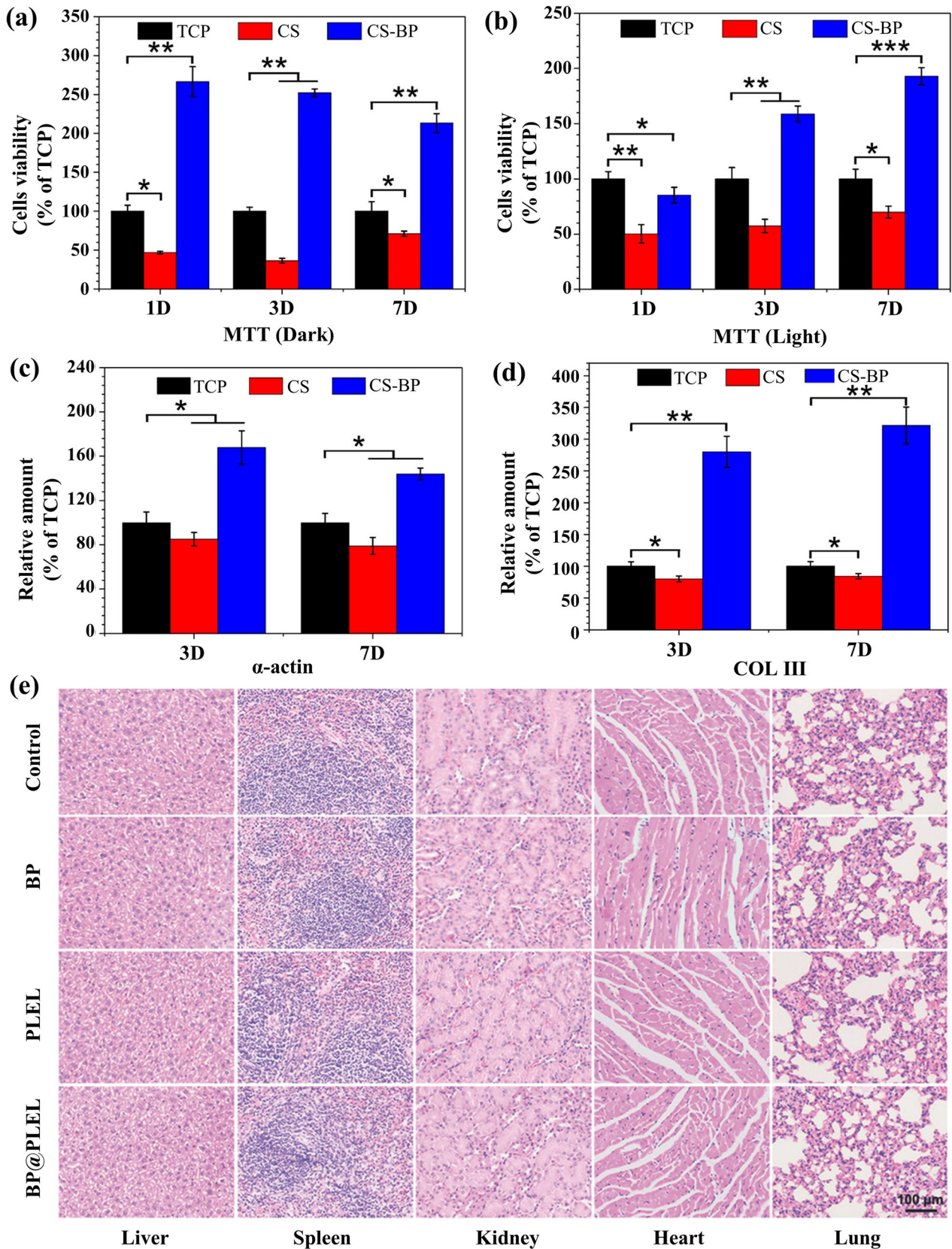
◄**Figure 6 a**, **b** Cell viabilities of the NIH-3T3 cells exposed to tissue culture plate (TCP), chitosan (CS) or chitosan-black phosphorus (CS-BP) hydrogel without (**a**) or with (**b**) initially irradiated for 10 min, and they were continuously co-cultured in the dark for 1, 3 and 7 days afterward. **c**, **d** Expressions of smooth muscle alpha actin (α-actin) gene (**c**) and collagen type III (COL III) gene (**d**) in NIH-3T3 cells (*$p < 0.05$, **$p < 0.01$, ***$p < 0.001$). Reproduced with permission from Ref. [96]. Copyright 2018, American Chemical Society. **e** Histological images of the liver, spleen, kidney, heart and lung of the mice that were injected with the BP nanosheets, [poly(d,l-lactide)-poly(ethylene glycol)-poly(d,l-lactide) (PDLLA-PEG-PDLLA: PLEL)] hydrogel and BP@PLEL hydrogel at 20 days post-injection. Reproduced with permission from Ref. [10]. Copyright 2018, WILEY.

impacts on the green algae (*Desmodesmus quadricauda*), two species of higher plants [sorghum (*Sorghum saccharatum*) and charlock (*Sinapis alba*)] were explored (Fig. 7b–f). The authors reported that the modification of Ti_3C_2 MXene with Al_2O_3 + Ag, SiO_2 + Ag and SiO_2 + Pd resulted in significant increases of antibacterial activities. The resultant nanomaterials caused both stimulating and inhibiting effects toward algae, which were depended on the concentration and the type of components. Yet, all the modifications resulted in a decrease in phytotoxicity toward the two plants in terms of sprout. The root growth of the plants was inhibited in the absence of $Ti_3C_2/Al_2O_3/Ag$ composites. The strongest inhibition of the seed germination (up to 40%) was observed in the group treated with Ti_3C_2 MXene [102].

As demonstrated above, the biosafety assessments of pg-2DMs-AA for the environmental safety or human health are summarized. However, more efforts are still needed in this direction and the following suggestions are given:

(1) Currently, dye-based colorimetric assays such as MTT assay are often utilized to determine the variations of cell viability in the in vitro assessment of pg-2DMs-AA. Yet, some reports suggest that MTT dyes might react with pg-2DMs such as MoS_2 and black phosphorous, causing perturbations to the final results [103, 104]. Therefore, to ensure the accuracies of assessment results, other approaches such as the electrical impedance spectroscopy can be utilized and compared with the colorimetric assays [105].

(2) The characteristics of the selected cells should be considered thoroughly for in vitro cytotoxicity assessment of pg-2DMs-AA. Different cell lines show different sensitivities to 2D material exposure [106, 107]. It has been shown that tumor cells are less sensitive to nanomaterials since they are more robust than the normal cells after all [108]. Therefore, we should be very careful in understanding the in vitro cytotoxicity results of pg-2DMs-AA which are based on some tumor cells such as HeLa cell.

(3) Cells response sensitively to the external stimulus at the molecular level and increasing reports explore the molecular events to fully evaluate the toxicities of nanomaterials [109, 110]. It will be more sensitive to decipher the biosafety of pg-2DMs-AA from RNA, protein and metabolite levels, which will be further supported by the high-throughput omics technologies [111].

(4) Little is known regarding the ecotoxicities of pg-2DMs-AA. As we known, the ecotoxicities of nanomaterials highly depend on their own physiochemical properties (e.g., size, thickness and component) [112]. Some insights regarding the ecotoxicities of pg-2DMs have already been obtained. Given that pg-2DMs-AA are quite different from their parent pg-2DMs in terms of physiochemical properties, the ecotoxicities of pg-2DMs-AA will be varied from those of pg-2DMs, and thus more efforts are needed in this direction.

Conclusion and perspective

Antibiotic-resistant bacteria have become a serious public health problem, causing a strong demand to develop novel agents with superior antimicrobial activities. The emergence of pg-2DMs with unique properties provides new alternatives to prepare antimicrobial agents. In this review, we summarized recent advances in the methods for boosting the antimicrobial activities of pg-2DMs-AA and evaluating the biosafety of pg-2DMs-AA. More excellent antimicrobial agents can be obtained based on pg-2DMs by incorporating more new approaches such as
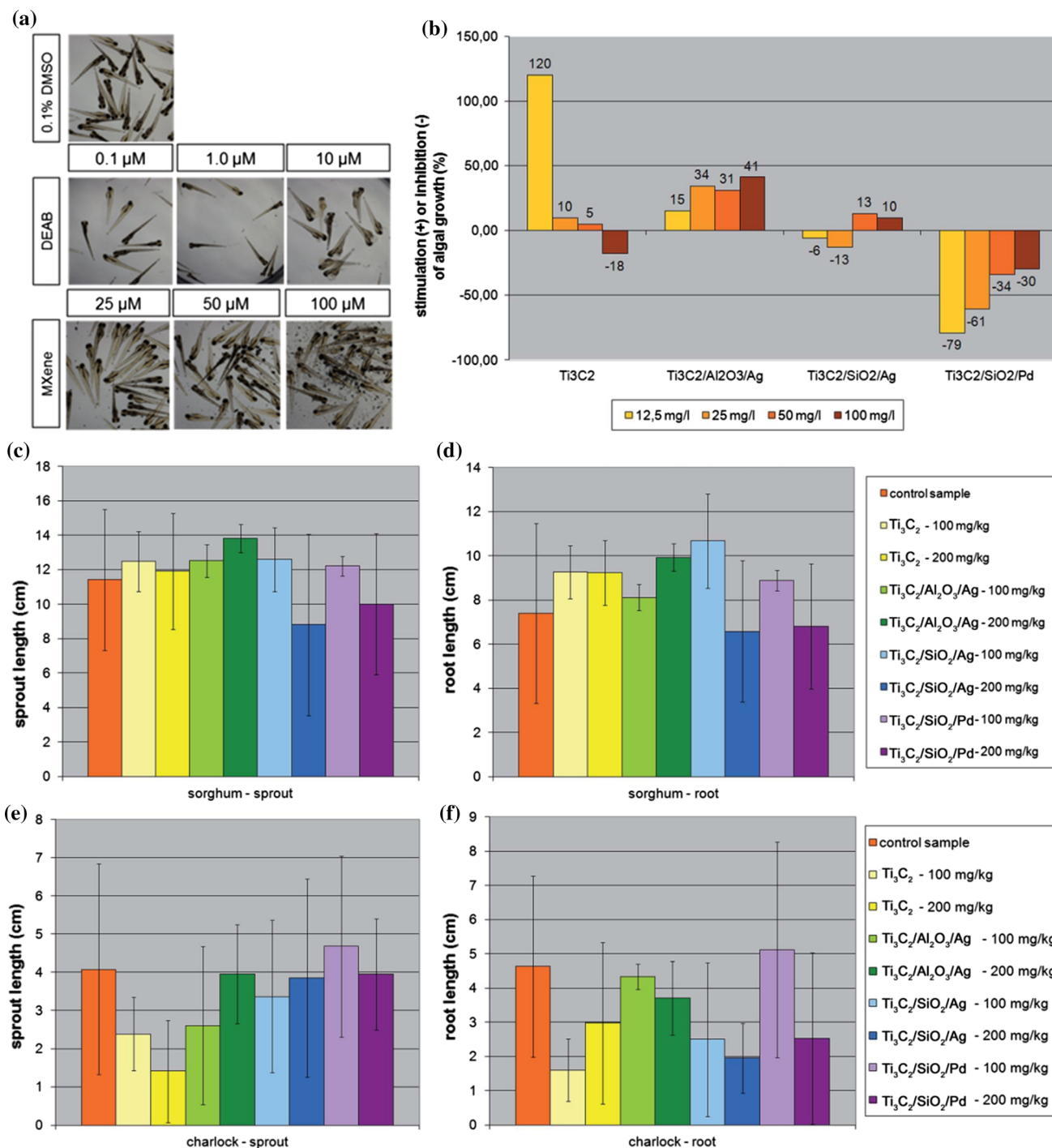
Figure 7 a Acute toxicity assessment of dimethyl sulfoxide (DMSO), diethylaminobenzaldehyde (DEAB) and Ti_3C_2Tx (MXene). Reproduced with permission from Ref. [101]. Copyright 2018, Royal Society of Chemistry. **b** Impacts of pristine Ti_3C_2MXene, $Ti_3C_2/Al_2O_3/Ag$, $Ti_3C_2/SiO_2/Ag$ and $Ti_3C_2/SiO_2/Pd$ nanocomposite on the algal growth after the incubation of 2 weeks. **c**–**f** The impacts of different nanopowders (100 mg/kg, 200 mg/kg) on the sprout length (**c**, **e**) and root length (**d**, **f**) of *Sorghum saccharatum* and *Sinapis alba*. Reproduced with permission from Ref. [102]. Copyright 2019, Royal Society of Chemistry.

phase engineer. Yet, the safety assessment should not be ignored as we expand the applications of pg-

2DMs-AA. More efforts are needed in this aspect, especially the ecological safety evaluation. All in all,

we believe pg-2DMs will provide more powerful weapons for the fight against pathogens.

Acknowledgements

References

[1] Rutledge-Taylor K, Matlow A, Gravel D et al (2012) A point prevalence survey of health care-associated infections in Canadian pediatric inpatients. Am J Infect Control 40:491–496

[2] Allegranzi B, Bagheri Nejad S, Combescure C, Graafmans W, Attar H, Donaldson L, Pittet D (2011) Burden of endemic health-care-associated infection in developing countries: systematic review and meta-analysis. Lancet 377:228–241

[3] Kraker MEAd, Stewardson AJ, Harbarth S (2016) Will 10 million people die a year due to antimicrobial resistance by 2050? PLoS Med 13:e1002184

[4] Beyth N, Houri-Haddad Y, Domb A, Khan W, Hazan R (2015) Alternative antimicrobial approach: nano-antimicrobial materials. Evid Based Complement Altern 2015:246012

[5] Miao H, Teng Z, Wang C, Chong H, Wang G (2019) Recent progress in two-dimensional antimicrobial nanomaterials. Chem Eur J 25:929–944

[6] Sun W, Wu F-G (2018) Two-dimensional materials for antimicrobial applications: graphene materials and beyond. Chem Asian J 13:3378–3410

[7] Zhang X, Zhang W, Liu L et al (2017) Antibiotic-loaded MoS_2 nanosheets to combat bacterial resistance via biofilm inhibition. Nanotechnology 28:225101

[8] Yuwen L, Sun Y, Tan G et al (2018) MoS_2@polydopamine-Ag nanosheets with enhanced antibacterial activity for effective treatment of *Staphylococcus aureus* biofilms and wound infection. Nanoscale 10:16711–16720

[9] Sun ZY, Zhang YQ, Yu H et al (2018) New solvent-stabilized few-layer black phosphorus for antibacterial applications. Nanoscale 10:12543–12553

[10] Shao JD, Ruan CS, Xie HH, Li ZB, Wang HY, Chu PK, Yu XF (2018) Black-phosphorus-incorporated hydrogel as a sprayable and biodegradable photothermal platform for postsurgical treatment of cancer. Adv Sci 5:1700848

[11] Yang QZ, Chang YY, Zhao HZ (2013) Preparation and antibacterial activity of lysozyme and layered double hydroxide nanocomposites. Water Res 47:6712–6718

[12] Rasool K, Mahmoud KA, Johnson DJ, Helal M, Berdiyorov GR, Gogotsi Y (2017) Efficient antibacterial membrane based on two-dimensional Ti_3C_2Tx (MXene) nanosheets. Sci Rep UK 7:1598

[13] Rasool K, Helal M, Ali A, Ren CE, Gogotsi Y, Mahmoud KA (2016) Antibacterial activity of Ti_3C_2Tx MXene. ACS Nano 10:3674–3684

[14] Meenakshisundaram I, Kalimuthu S, Priya PG, Karthikeyan S (2019) Facile green synthesis and antimicrobial performance of Cu_2O nanospheres decorated g-C_3N_4 nanocomposite. Mater Res Bull 112:331–335

[15] Zhao HX, Yu HT et al (2014) Fabrication of atomic single layer graphitic-C_3N_4 and its high performance of photocatalytic disinfection under visible light irradiation. Appl Catal B Environ 152:46–50

[16] Zhu C, Shen H, Liu H, Lv X, Li Z, Yuan Q (2018) Solution-processable two-dimensional In_2Se_3 nanosheets as efficient photothermal agents for elimination of bacteria. Chemistry 24:19060–19065

[17] Francois P, Andreia Fonseca DF, Siamak N, Menachem EJAN (2015) Antimicrobial properties of graphene oxide nanosheets: why size matters. ACS Nano 9:7226–7236

[18] Shaobin L, Ming H, Tingying Helen Z et al (2012) Lateral dimension-dependent antibacterial activity of graphene oxide sheets. Langmuir 28:12364–12372

[19] Yang X, Li J, Liang T et al (2014) Antibacterial activity of two-dimensional MoS_2 sheets. Nanoscale 6:10126–10133

[20] Mak KF, Lee C, Hone J, Shan J, Heinz TF (2010) Atomically thin MoS_2: a new direct-gap semiconductor. Phys Rev Lett 105:136805

[21] Zhang Y, Chang TR, Zhou B et al (2014) Direct observation of the transition from indirect to direct bandgap in atomically thin epitaxial $MoSe_2$. Nat Nanotechnol 9:111–115

[22] Novoselov KS, Geim AK, Morozov SV et al (2004) Electric field effect in atomically thin carbon films. Science 306:666–669

[23] Hai L, Jumiati W, Zongyou Y, Hua ZJACR (2014) Preparation and applications of mechanically exfoliated single-

layer and multilayer MoS$_2$ and WSe$_2$ nanosheets. Acc Chem Res 47:1067–1075

[24] Feng Z, Liu X, Tan L et al (2018) Electrophoretic deposited stable Chitosan@MoS$_2$ coating with rapid in situ bacteria-killing ability under dual-light irradiation. Small 14:1704347

[25] Zhang W, Shi S, Wang Y et al (2016) Versatile molybdenum disulfide based antibacterial composites for in vitro enhanced sterilization and in vivo focal infection therapy. Nanoscale 8:11642–11648

[26] Pérez-Martínez P, Galvan-Miyoshi JM, Ortiz-López J (2016) Ultrasonic cavitation effects on the structure of graphene oxide in aqueous suspension. J Mater Sci 51:10782–10792. https://doi.org/10.1007/s10853-016-0290-0

[27] Niu LY, Coleman JN, Zhang H, Shin H, Chhowalla M, Zheng ZJ (2016) Production of two-dimensional nanomaterials via liquid-based direct exfoliation. Small 12:272–293

[28] Muscuso L, Cravanzola S, Cesano F, Scarano D, Zecchina A (2015) Optical, vibrational, and structural properties of MoS$_2$ nanoparticles obtained by exfoliation and fragmentation via ultrasound cavitation in isopropyl alcohol. J Phys Chem C 119:3791–3801

[29] Han GQ, Liu YR, Hu WH et al (2015) WS$_2$ nanosheets based on liquid exfoliation as effective electrocatalysts for hydrogen evolution reaction. Mater Chem Phys 167:271–277

[30] Smith RJ, King PJ, Lotya M et al (2011) Large-scale exfoliation of inorganic layered compounds in aqueous surfactant solutions. Adv Mater 23:3944–3948

[31] Tan L, Li J, Liu XM et al (2018) In situ disinfection through photoinspired radical oxygen species storage and thermal-triggered release from black phosphorous with strengthened chemical stability. Small 14:1703197

[32] Paredes JI, Villar-Rodil S (2016) Biomolecule-assisted exfoliation and dispersion of graphene and other two-dimensional materials: a review of recent progress and applications. Nanoscale 8:15389–15413

[33] Cai X, Luo Y, Liu B, Cheng HM (2018) Preparation of 2D material dispersions and their applications. Chem Soc Rev 47:6224–6266

[34] Bang GS, Cho S, Son N, Shim GW, Cho BK, Choi SY (2016) DNA-assisted exfoliation of tungsten dichalcogenides and their antibacterial effect. ACS Appl Mater Interfaces 8:1943–1950

[35] Huang XW, Wei JJ, Liu T, Zhang XL, Bai SM, Yang HH (2017) Silk fibroin-assisted exfoliation and functionalization of transition metal dichalcogenide nanosheets for antibacterial wound dressings. Nanoscale 9:17193–17198

[36] Cao W, Yue L, Wang Z (2019) High antibacterial activity of chitosan–molybdenum disulfide nanocomposite. Carbohyd Polym 215:226–234

[37] Chou SS, De M, Kim J et al (2013) Ligand conjugation of chemically exfoliated MoS$_2$. J Am Chem Soc 135:4584–4587

[38] Pandit S, Karunakaran S, Boda SK, Basu B, De M (2016) High antibacterial activity of functionalized chemically exfoliated MoS$_2$. ACS Appl Mater Interfaces 8:31567–31573

[39] Karunakaran S, Pandit S, Basu B, De M (2018) Simultaneous exfoliation and functionalization of 2H-MoS$_2$ by thiolated surfactants: applications in enhanced antibacterial activity. J Am Chem Soc 140:12634–12644

[40] Murugan C, Sharma V, Murugan RK, Malaimegu G, Sundaramurthy A (2019) Two-dimensional cancer theranostic nanomaterials: synthesis, surface functionalization and applications in photothermal therapy. J Control Release 299:1–20

[41] Chen CS, Yu WW, Liu TG, Cao SY, Tsang YH (2017) Graphene oxide/WS$_2$/Mg-doped ZnO nanocomposites for solar-light catalytic and anti-bacterial applications. Sol Energy Mater Sol Cells 160:43–53

[42] Pandit S, Cao Z, Mokkapati VRSS et al (2018) Vertically aligned graphene coating is bactericidal and prevents the formation of bacterial biofilms. Adv Mater Interfaces 5:1701331

[43] Lu XL, Feng XD, Werber JR et al (2017) Enhanced antibacterial activity through the controlled alignment of graphene oxide nanosheets. Proc Natl Acad Sci USA 114:E9793–E9801

[44] Szunerits S, Boukherroub R (2016) Antibacterial activity of graphene-based materials. J Mater Chem B 4:6892–6912

[45] Liu C, Kong D, Hsu PC et al (2016) Rapid water disinfection using vertically aligned MoS$_2$ nanofilms and visible light. Nat Nanotechnol 11:1098–1104

[46] Alimohammadi F, Sharifian MG, Attanayake NH, Thenuwara AC, Gogotsi Y, Anasori B, Strongin DR (2018) Antimicrobial properties of 2D MnO$_2$ and MoS$_2$ nanomaterials vertically aligned on graphene materials and Ti$_3$C$_2$ MXene. Langmuir 34:7192–7200

[47] Liu Z, Wang XH, Qiao P, Tian Y, Li HJ, Yang J (2015) Uniformed polyaniline supported MoS$_2$ nanorod: a photocatalytic hydrogen evolution and anti-bacteria material. J Mater Sci Mater Electron 26:7153–7158

[48] Tang K, Wang L, Geng H, Qiu J, Cao H, Liu X (2017) Molybdenum disulfide (MoS$_2$) nanosheets vertically coated on titanium for disinfection in the dark. Arab J Chem 13:1612–1623

[49] Wu YX, Xu MQ, Chen X, Yang SL, Wu HS, Pan J, Xiong X (2016) CTAB-assisted synthesis of novel ultrathin MoSe$_2$ nanosheets perpendicular to graphene for the adsorption and photodegradation of organic dyes under visible light. Nanoscale 8:440–450

[50] Liu S, Liu Y, Lei WW, Zhou X, Xu K, Qiao QQ, Zhang WH (2018) Few-layered ReS$_2$ nanosheets vertically aligned on reduced graphene oxide for superior lithium and sodium storage. J Mater Chem A 6:20267–20276

[51] Yeonwoong J, Jie S, Yong S, Cha JJ (2014) Chemically synthesized heterostructures of two-dimensional molybdenum/tungsten-based dichalcogenides with vertically aligned layers. ACS Nano 8:9550–9557

[52] Jie Y, Li Q, Yufeng H et al (2010) Vertically aligned boron nitride nanosheets: chemical vapor synthesis, ultraviolet light emission, and superhydrophobicity. ACS Nano 4:414–422

[53] Wang S, Zhang HJ, Zhang D, Ma Y, Bi XF, Yang SB (2018) Vertically oriented growth of MoO$_3$ nanosheets on graphene for superior lithium storage. J Mater Chem A 6:672–679

[54] Yu WL, Chen JX, Shang TT, Chen LF, Gu L, Peng TY (2017) Direct Z-scheme g-C$_3$N$_4$/WO$_3$ photocatalyst with atomically defined junction for H-2 production. Appl Catal B Environ 219:693–704

[55] Xia Y, Mathis TS, Zhao MQ et al (2018) Thickness-independent capacitance of vertically aligned liquid-crystalline MXenes. Nature 557:409–412

[56] Li RN, Xue TS, Bingre R, Gao YS, Louis B, Wang Q (2018) Microporous zeolite@vertically aligned Mg-Al layered double hydroxide core@shell structures with improved hydrophobicity and toluene adsorption capacity under wet conditions. ACS Appl Mater Interfaces 10:34834–34839

[57] Xing HN, Lan YY, Zong Y, Sun Y, Zhu XH, Li XH, Zheng XL (2019) Ultrathin NiCo-layered double hydroxide nanosheets arrays vertically grown on Ni foam as binder-free high-performance supercapacitors. Inorg Chem Commun 101:125–129

[58] Ganguly P, Byrne C, Breen A, Pillai SC (2018) Antimicrobial activity of photocatalysts: fundamentals, mechanisms, kinetics and recent advances. Appl Catal B Environ 225:51–75

[59] An T, Zhao H, Wong PK (2017) Advances in photocatalytic disinfection. Springer, Berlin

[60] Tian X, Sun Y, Fan S, Boudreau MD, Chen C, Ge C, Yin JJ (2019) Photogenerated charge carriers in molybdenum disulfide quantum dots with enhanced antibacterial activity. ACS Appl Mater Interfaces 11:4858–4866

[61] Priyadharsan A, Shanavas S, Vasanthakumar V, Balamuralikrishnan B, Anbarasan PM (2018) Synthesis and investigation on synergetic effect of rGO-ZnO decorated MoS$_2$ microflowers with enhanced photocatalytic and antibacterial activity. Colloid Surf A 559:43–53

[62] Jo WK, Selvam NCS (2015) Enhanced visible light-driven photocatalytic performance of ZnO-g-C$_3$N$_4$ coupled with graphene oxide as a novel ternary nanocomposite. J Hazard Mater 299:462–470

[63] Habibi-Yangjeh A, Akhundi A (2016) Novel ternary g-C$_3$N$_4$/Fe$_3$O$_4$/Ag$_2$CrO$_4$ nanocomposites: magnetically separable and visible-light-driven photocatalysts for degradation of water pollutants. J Mol Catal A Chem 415:122–130

[64] Lam SM, Sin JC, Mohamed AR (2016) A review on photocatalytic application of g-C$_3$N$_4$/semiconductor (CNS) nanocomposites towards the erasure of dyeing wastewater. Mater Sci Semicond Proc 47:62–84

[65] Liu Y, Zeng XK, Hu XY, Hu J, Zhang XW (2019) Two-dimensional nanomaterials for photocatalytic water disinfection: recent progress and future challenges. J Chem Technol Biotechnol 94:22–37

[66] Li Z, Meng X, Zhang Z (2018) Recent development on MoS$_2$-based photocatalysis: A review. J Photochem Photobiol C 35:39–55

[67] Han B, Hu YH (2016) MoS$_2$ as a co-catalyst for photocatalytic hydrogen production from water. Energy Sci Eng 4:285–304

[68] Parzinger E, Miller B, Blaschke B, Garrido JA, Ager JW, Holleitner A, Wurstbauer U (2015) Photocatalytic stability of single- and few-layer MoS$_2$. ACS Nano 9:11302–11309

[69] Chang K, Mei ZW, Wang T, Kang Q, Ouyang SX, Ye JH (2014) MoS$_2$/graphene cocatalyst for efficient photocatalytic H$_2$ evolution under visible light irradiation. ACS Nano 8:7078–7087

[70] Wang TQ, Sun MZ, Sun HL, Shang J, Wong PK (2019) Efficient Z-scheme visible-light-driven photocatalytic bacterial inactivation by hierarchical MoS$_2$-encapsulated hydrothermal carbonation carbon core-shell nanospheres. Appl Surf Sci 464:43–52

[71] Feng Y, Liu L, Zhang J, Aslan H, Dong M (2017) Photoactive antimicrobial nanomaterials. J Mater Chem B 5:8631–8652

[72] Miao Z, Fan L, Xie X, Ma Y, Xue J, He T, Zha Z (2019) Liquid exfoliation of atomically thin antimony selenide as an efficient two-dimensional antibacterial nanoagent. ACS Appl Mater Interfaces 11:26664–26673

[73] Xu JW, Yao K, Xu ZK (2019) Nanomaterials with a photothermal effect for antibacterial activities: an overview. Nanoscale 11:8680–8691

[74] Liu G, Zou J, Tang Q et al (2017) Surface modified Ti_3C_2 MXene nanosheets for tumor targeting photothermal/photodynamic/chemo synergistic Therapy. ACS Appl Mater Interfaces 9:40077–40086

[75] Ma K, Li Y, Wang Z et al (2019) Core–shell gold nanorod@layered double hydroxide nanomaterial with highly efficient photothermal conversion and its application in antibacterial and tumor therapy. ACS Appl Mater Interfaces 11:29630–29640

[76] Lin Y, Han D, Li Y et al (2019) Ag_2S@ WS_2 heterostructure for rapid bacteria-killing using near-infrared light. ACS Sustain Chem Eng 7:14982–14990

[77] Yang GC, Liu ZM, Li Y et al (2017) Facile synthesis of black phosphorus-Au nanocomposites for enhanced photothermal cancer therapy and surface-enhanced Raman scattering analysis. Biomater Sci UK 5:2048–2055

[78] Ma M, Liu X, Tan L et al (2019) Enhancing the antibacterial efficacy of low-dose gentamicin with 5 minute assistance of photothermy at 50 degrees C. Biomater Sci UK 7:1437–1447

[79] Li MX, Sultanbawa Y, Xu ZP, Gu WY, Chen WY, Liu JY, Qian GR (2019) High and long-term antibacterial activity against Escherichia coli via synergy between the antibiotic penicillin G and its carrier ZnAl layered double hydroxide. Colloid Surface B 174:435–442

[80] Komarala EP, Doshi S, Thiyagarajan S, Aslam M, Bahadur D (2018) Studies on drug release kinetics and antibacterial activity against drug-resistant bacteria of cefotaxime sodium loaded layered double hydroxide-fenugreek nanohybrid. New J Chem 42:129–136

[81] Tang LP, Cheng HM, Cui SM, Wang XR, Song LY, Zhou W, Li SJ (2018) DL-mandelic acid intercalated Zn-Al layered double hydroxide: a novel antimicrobial layered material. Colloid Surface B 165:111–117

[82] Mishra G, Dash B, Pandey S, Mohanty PP (2013) Antibacterial actions of silver nanoparticles incorporated Zn-Al layered double hydroxide and its spinel. J Environ Chem Eng 1:1124–1130

[83] Bouaziz Z, Soussan L, Janot JM et al (2017) Structure and antibacterial activity relationships of native and amyloid fibril lysozyme loaded on layered double hydroxide. Colloid Surface B 157:10–17

[84] Chang K, Hai X, Pang H et al (2016) Targeted synthesis of 2H-and 1T-phase MoS_2 monolayers for catalytic hydrogen evolution. Adv Mater 28:10033–10041

[85] Liu L, Wu J, Wu L et al (2018) Phase-selective synthesis of 1T' MoS_2 monolayers and heterophase bilayers. Nat Mater 17:1108–1114

[86] Voiry D, Salehi M, Silva R et al (2013) Conducting MoS_2 nanosheets as catalysts for hydrogen evolution reaction. Nano Lett 13:6222–6227

[87] Lukowski MA, Daniel AS, Meng F, Forticaux A, Li L, Jin S (2013) Enhanced hydrogen evolution catalysis from chemically exfoliated metallic MoS_2 nanosheets. J Am Chem Soc 135:10274–10277

[88] Guiney LM, Wang X, Xia T, Nel AE, Hersam MC (2018) Assessing and mitigating the hazard potential of two-dimensional materials. ACS Nano 12:6360–6377

[89] Fojtu M, Teo WZ, Pumera M (2017) Environmental impact and potential health risks of 2D nanomaterials. Environ Sci Nano 4:1617–1633

[90] Pandit S, Karunakaran S, Boda SK, Basu B, De M (1944) High antibacterial activity of functionalized chemically exfoliated MoS_2. ACS Appl Mater Interfaces 8:31567–31573

[91] Yin W, Yu J, Lv F, Yan L, Zheng LR, Gu Z, Zhao Y (2016) Functionalized nano-MoS_2 with peroxidase catalytic and near-infrared photothermal activities for safe and synergetic wound antibacterial applications. ACS Nano 10:11000–11011

[92] Wang ZZ, Dong K, Liu Z et al (2017) Activation of biologically relevant levels of reactive oxygen species by Au/g-C_3N_4 hybrid nanozyme for bacteria killing and wound disinfection. Biomaterials 113:145–157

[93] Chakraborti M, Jackson JK, Plackett D, Gilchrist SE, Burt HM (2012) The application of layered double hydroxide clay (LDH)-poly(lactide-co-glycolic acid) (PLGA) film composites for the controlled release of antibiotics. J Mater Sci Mater Med 23:1705–1713

[94] Pal A, Jana TK, Roy T, Pradhan A, Maiti R, Choudhury SM, Chatterjee K (2018) MoS_2–TiO_2 nanocomposite with excellent adsorption performance and high antibacterial activity. Chemistryselect 3:81–90

[95] Marcato PD, Parizotto NV, Martinez DST et al (2013) New hybrid material based on layered double hydroxides and biogenic silver nanoparticles: antimicrobial activity and cytotoxic effect. J Brazil Chem Soc 24:266–272

[96] Mao CY, Xiang YM, Liu XM et al (2018) Repeatable photodynamic therapy with triggered signaling pathways of fibroblast cell proliferation and differentiation to promote bacteria-accompanied wound healing. ACS Nano 12:1747–1759

[97] Zhang W, Mou Z, Wang Y et al (2019) Molybdenum disulfide nanosheets loaded with chitosan and silver nanoparticles effective antifungal activities: in vitro and in vivo. Mater Sci Eng C Mater 7:486–497

[98] Eguchi K, Nagase H, Ozawa M et al (2004) Evaluation of antimicrobial agents for veterinary use in the ecotoxicity test using microalgae. Chemosphere 57:1733–1738

[99] Galdiero E, Siciliano A, Maselli V et al (2016) An integrated study on antimicrobial activity and ecotoxicity of quantum dots and quantum dots coated with the antimicrobial peptide indolicidin. Int J Nanomed 11:4199–4211

[100] Ma H, Williams PL, Diamond SA (2013) Ecotoxicity of manufactured ZnO nanoparticles—a review. Environ Pollut 172:76–85

[101] Nasrallah GK, Al-Asmakh M, Rasool K, Mahmoud KA (2018) Ecotoxicological assessment of Ti_3C_2Tx (MXene) using a zebrafish embryo model. Environ Sci Nano 5:1002–1011

[102] Rozmyslowska-Wojciechowska A, Karwowska E, Pozniak S, Wojciechowski T et al (2019) Influence of modification of Ti_3C_2 MXene with ceramic oxide and noble metal nanoparticles on its antimicrobial properties and ecotoxicity towards selected algae and higher plants. RSC Adv 9:4092–4105

[103] Chng ELK, Sofer Z, Pumera M (2014) MoS_2 exhibits stronger toxicity with increased exfoliation. Nanoscale 6:14412–14418

[104] Latiff NM, Teo WZ, Sofer Z, Fisher AC, Pumera M (2015) The cytotoxicity of layered black phosphorus. Chem Eur J 21:13991–13995

[105] Shah P, Narayanan TN, Li CZ, Alwarappan S (2015) Probing the biocompatibility of MoS_2 nanosheets by cytotoxicity assay and electrical impedance spectroscopy. Nanotechnology 26:315102

[106] Qu G, Liu W, Zhao Y et al (2017) Improved biocompatibility of black phosphorus nanosheets by chemical modification. Angew Chem 56:14488–14493

[107] Zhang X, Zhang Z, Zhang S et al (2017) Size effect on the cytotoxicity of layered black phosphorus and underlying mechanisms. Small 13:1701210

[108] Li Z, Yang R, Yu M, Bai F, Li C, Wang ZL (2008) Cellular level biocompatibility and biosafety of ZnO nanowires. J Phys Chem C 112:20114–20117

[109] Lu XY, Huang Y, Yu YD, Yang YM (2013) Application of genomics/proteomics technologies in the research of biocompatibility of biomaterials. J Inorg Mater 28:21–28

[110] Caballero Díaz E, Cases M (2016) Analytical methodologies for nanotoxicity assessment. TrAC Trends Anal Chem 84:160–171

[111] Frohlich E (2017) Role of omics techniques in the toxicity testing of nanoparticles. J Nanobiotechnol 15:84

[112] Klaine SJ, Alvarez PJ, Batley GE et al (2008) Nanomaterials in the environment: behavior, fate, bioavailability, and effects. Environ Toxicol Chem 27:1825–1851